molecule. This is fully consistent with our earlier studies of halogenated epoxides[17] and can be attributed to the greater charge capacity of chlorine.[18]

The most striking change in going from I and II, which are inactive with respect to receptor binding, AHH induction, and toxicity, to the highly active and toxic TCDD is the drastic weakening of the oxygen negative potentials. Figure 3 presents this from another perspective, showing the very extensive and strong negative regions in I shrinking to the small and weak ones that are found in TCDD.

The presence of relatively strong negative potentials along the entire lateral regions of TCDD and their absence or lesser presence in the other four inactive or marginally active molecules suggest that negative lateral regions of a certain minimum strength may play an essential role in the interaction with the receptor. The experimental observation that activity requires at least three halogen substituents on these sites reinforces this view, since the electron-attracting halogens do give rise to negative regions. These are stronger in the case of chlorine than fluorine, which is consistent with the observed greater potency of chlorine in inducing activity. We also speculate that the weakening of the negative region above the oxygens may be a contributing factor to increasing activity.

(18) (a) Huheey, J. E. *J. Phys. Chem.* **1965**, *69*, 3284. (b) Evans, R. S.; Huheey, J. E. *Chem. Phys. Lett.* **1973**, *19*, 114. (c) Politzer, P. "Homoatomic Rings, Chains and Macromolecules of Main-Group Elements"; Rheingold, A. L., Ed.; Elsevier: New York, 1977; Chapter 4.

Acknowledgment. We express our appreciation to the US Environmental Protection Agency for partial funding of this work under assistance agreement CR 808866-01-0 to Peter Politzer. The contents do not necessarily reflect the views and policies of the Environmental Protection Agency, nor does mention of trade names or commercial products constitute endorsement or recommendation for use. We are also grateful for the financial support provided by the University of New Orleans Computer Research Center.

Complete Proton and Carbon-13 NMR Assignment of the Alkaloid Gephyrotoxin through the Use of Homonuclear Hartmann–Hahn and Two-Dimensional NMR Spectroscopy

Michael W. Edwards and Ad Bax*

Contribution from the Laboratory of Bioorganic Chemistry and Laboratory of Chemical Physics, National Institute of Arthritis, Diabetes, and Digestive and Kidney Diseases, National Institutes of Health, Bethesda, Maryland 20892. *Received September 9, 1985*

Abstract: Three different types of modern NMR techniques have been used to obtain a complete proton and carbon-13 assignment of the alkaloid gephyrotoxin. In addition to the two-dimensional phase-sensitive homo- and heteronuclear shift correlation methods, use of the recently proposed one-dimensional homonuclear Hartmann–Hahn difference experiment was crucial for obtaining the required long-range connectivity. Guidelines are presented for optimal use of these techniques. Experiments were performed at 500-MHz ^1H frequency, using 8 mg of sample.

The introduction of two-dimensional (2D) NMR techniques has greatly simplified the NMR analysis of many natural products, permitting the study of problems hitherto considered intractable. As an example, we present here a study of the alkaloid gephyrotoxin (GyTx), extracted from the skin of the frog *Dendrobates histrionicus*. Routine application of standard 2D NMR techniques is not sufficient in this case because of the complexity of the ^1H spectrum in the methylene region. A second limitation is imposed by the small amount of sample available, which prohibits the application of most of the more advanced, but less sensitive, ^{13}C NMR experiments.

Frogs of the family Dendrobatid produce a wide range of unique alkaloids.[1,2] Many of the alkaloids exhibit pharmacological activity on nerve and muscle.[3,4] These alkaloids have been categorized by structural similarities into five major classes: the batrachotoxins, the histrionicotoxins, the gephyrotoxins, and the pumiliotoxin C and pumiliotoxin A classes. Gephyrotoxin (GyTx), a major alkaloid of the perhydrobenzoindolizidine-type structure, is a tricyclic compound with the empirical formula $C_{19}H_{29}NO_4$ (I). There has, to the best of our knowledge, been no successful attempt at establishing the complete ^1H and ^{13}C NMR assignment of GyTx. The present effort is to identify the proton and carbon resonances of this biologically active compound[5,6] as a reference for isotopic labeling studies and to add to the database of alkaloids derived from amphibians, which may aid in the structural elucidation of new alkaloids of unknown structure. The strategy for complete assignment is to use the newly developed HOHAHA relay experiment[7] along with standard homo- and heteronuclear two-dimensional shift correlation techniques. Special attention is paid to the experimental optimization of the various NMR experiments, both from the resolution and sensitivity points of view.

Experimental Approach

Double-Quantum Filtered COSY. The first step in the NMR analysis of GyTx is the recording of a ^1H–^1H connectivity map. Because of the high resolution provided by the double-quantum filtered[8] absorption mode[9,10] COSY method, this technique is

* Address correspondence to this author at the Laboratory of Chemical Physics.

(1) Daly, J. W.; Witkop, B.; Tokuyama, T.; Nishikawa, T.; Karle, I. L. *Helv. Chim. Acta* **1977**, *60*, 1128–1140.
(2) Daly, J. W.; Brown, G. B.; Mensa Dwumah, M.; Myers, C. W. *Toxicon* **1978**, *16*, 163–188.
(3) Lapa, A. J.; Albuquerque, E. X.; Sarvey, J. M.; Daly, J.; Witkop, B. *Exp. Neurol.* **1975**, *47*, 558–578.
(4) Eldefrawi, M. E.; Eldefrawi, A. T.; Mansour, N. A.; Daly, J.; Witkop, B.; Albuquerque, E. X. *Biochemistry* **1978**, *17*, 5474–5484.
(5) Souccar, C.; Varanda, W. A.; Aronstam, R. S.; Daly, J. W.; Albuquerque, E. X. *Mol. Pharmacol.* **1984**, *25*, 395–400.
(6) Souccar, C.; Varanda, W. A.; Daly, J. W.; Albuquerque, E. X. *Mol. Pharmacol.* **1984**, *25*, 384–394.
(7) Davis, D. G.; Bax, A. *J. Am. Chem. Soc.* **1985**, *107*, 7197–7198.
(8) Piantini, U.; Sorensen, O. W.; Ernst, R. R. *J. Am. Chem. Soc.* **1982**, *104*, 6800–6801.

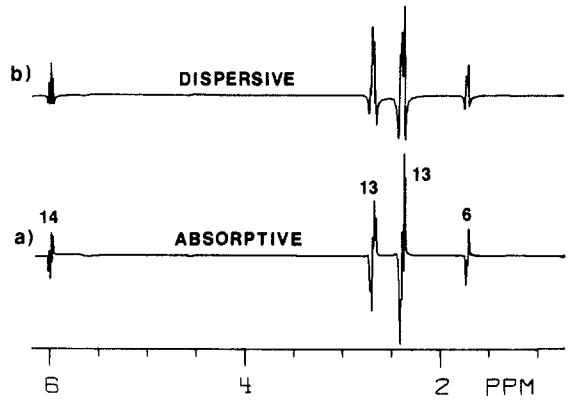

Figure 1. (a) Absorptive and (b) dispersive phasing of a section through the double-quantum filtered COSY spectrum parallel to the F_1 axis, taken at the F_2 frequency of the H13 multiplet.

preferable to the regular COSY method.[11-13] However, the extensive phase cycling required in the double-quantum filtered absorption experiment necessarily leads to long minimum measuring times, which is a disadvantage of the method. Before the spectrum obtained with this method is presented, some important practical details of the experiment will be discussed briefly.

In the double-quantum filtered version of the COSY experiment, a 90° pulse is added to the standard sequence, resulting in 90_ϕ–t_1–90_ψ–90_θ–acquire(t_2). Phase cycling of the final pulse (or of the first two pulses) permits one to detect exclusively signals that originate from double-quantum coherence, present after the second 90° pulse[14,15] (see Experimental Section). To permit recording of the spectrum in the 2D absorption mode and simultaneously separate positive and negative modulation frequencies, the sine- and cosine-modulated signals (usually corresponding to the odd- and even-numbered scans) are stored in separate locations in memory. Data processing then proceeds in the standard fashion.[16-18] Alternatively, the time-proportional-phase-incrementation (TPPI) approach can be used,[10] leading to identical results at the same expense of data storage space and data acquisition time. Practical problems may occur in phasing the 2D spectrum to the absorption mode. First, for $t_1 = 0$, no double-quantum coherence exists after the second 90° pulse and consequently zero intensity is obtained for the spectrum recorded for $t_1 = 0$. Hence, this spectrum cannot be used for phase adjustment. For larger values of t_1, transverse magnetization that originates from double-quantum coherence and that has been transferred from one proton to another will be aligned along the $\pm x$ axis after a 90_x pulse[19] (and along the $\pm y$ axis after a 90_y pulse). These signals are 90° out of phase relative to signals detected in a regular one-dimensional experiment after a 90_x pulse (or a 90_y pulse). Correct phasing in the F_2 dimension of the 2D spectrum is therefore obtained if the phasing parameters used are those needed to phase the regular one-dimensional spectrum to the purely *dispersive* mode. Note that if a certain proton is coupled to more than one other proton, the diagonal multiplet in the

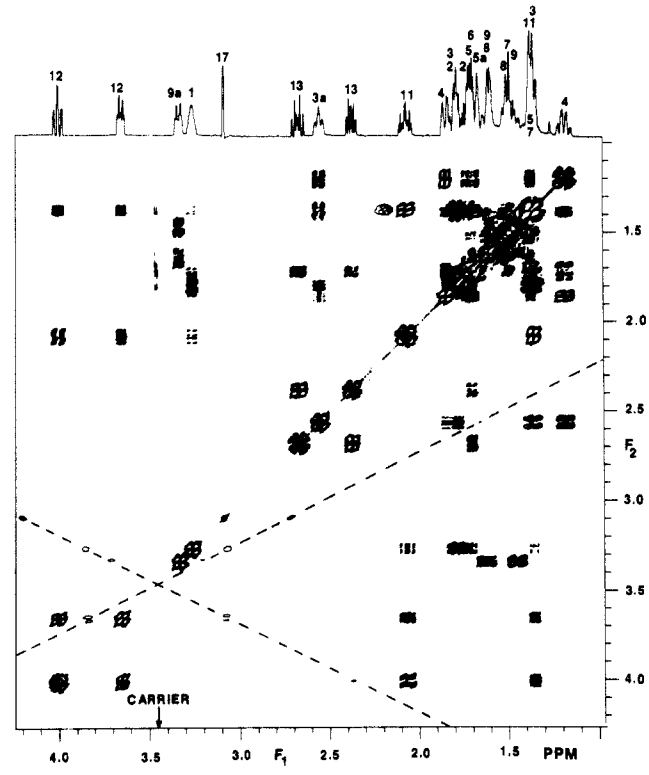

Figure 2. 500-MHz double-quantum filtered COSY spectrum of GyTx. Both positive and negative contours are shown. Only the high-field region of the spectrum is shown. The carrier was positioned at 3.45 ppm. Low intensity artifacts, caused by too high an experiment repetition rate, are observed on the lines $F_1 = NF_2$ ($N = -2, -1, 0, 1, 2$). The "double-quantum diagonals", $F_1 = \pm 2F_2$, are drawn as dashed lines in the spectrum.

double-quantum filtered COSY spectrum will contain some antiphase dispersive components, additional to the antiphase absorptive components. After transposition of the data matrix and Fourier transformation in the t_1 dimension, correct F_1 phasing is obtained by selecting a cross section through a multiplet (not taken at the center of this multiplet) of a proton that is coupled to at least one other proton that differs significantly (several ppm) in chemical shift. Because of the antiphase nature of the multiplet components, the cross section is absorptively phased when one-half of the components of each cross-multiplet points up and the other half points down (Figure 1a). The dispersive part of the spectrum (Figure 1b) may at first sight appear rather similar to regular absorption mode phasing. This is due to the antiphase nature of the dispersive multiplet components and provides less resolution than the absorption mode phasing. The phasing procedure in the F_2 dimension is only valid if the final pulse has a flip angle close to 90°; for flip angles different from 90°, F_2 phasing is obtained by adjustment of a spectrum obtained for a t_1 value of about 15 ms. In this case, absorptive phasing will show the multiplet shape of Figure 1a, and dispersive phasing shows a symmetric dip around the center of the multiplet, as visible in Figure 1b.

The regular one-dimensional 500-MHz ^1H spectrum of GyTx shows severe spectral overlap in the 1.3–1.8-ppm region, which is partially removed in the absorption mode double-quantum filtered COSY spectrum (Figure 2). Details on the recording of this spectrum are given in the Experimental Section. A number of ^1H resonance assignments can be made from this spectrum. Assignment of protons in the conjugated ring systems, however, is not directly feasible on the basis of this spectrum alone and requires connectivity through more than three bonds. Attempts to use single and multiple homonuclear relayed magnetization transfer[20-22] (data not shown) were only partly successful in ob-

(9) Rance, M.; Sorensen, O. W.; Bodenhausen, G.; Wagner, G.; Ernst, R. R.; Wüthrich, K. *Biochem. Biophys. Res. Commun.* **1983**, *117*, 479–485.
(10) Marion, D.; Wüthrich, K. *Biochem. Biophys. Res. Commun.* **1983**, *113*, 967–974.
(11) Aue, W. P.; Bartholdi, E.; Ernst, R. R. *J. Chem. Phys.* **1976**, *64*, 2229–2242.
(12) Bax, A.; Freeman, R. *J. Magn. Reson.* **1981**, *44*, 542–561.
(13) Nagayama, K.; Kumar, A.; Wüthrich, K.; Ernst, R. R. *J. Magn. Reson.* **1980**, *40*, 321–334.
(14) Wokaun, A.; Ernst, R. R. *Chem. Phys. Lett.* **1977**, *52*, 407–412.
(15) Bax, A.; Kempsell, S.; Freeman, R. *J. Am. Chem. Soc.* **1980**, *102*, 4849–4851.
(16) Müller, L.; Ernst, R. R. *Mol. Phys.* **1979**, *38*, 963–992.
(17) States, D. J.; Haberkorn, R. A.; Ruben, D. J. *J. Magn. Reson.* **1982**, *48*, 286–292.
(18) Bax, A. *Bull. Magn. Reson.* **1985**, *7*, 167–183.
(19) Bax, A. "Two-dimensional Nuclear Magnetic Resonance in Liquids"; Reidel: Boston, 1982; pp 157–158.
(20) Eich, G.; Bodenhausen, G.; Ernst, R. R. *J. Am. Chem. Soc.* **1982**, *104*, 3732–3733.
(21) Bax, A.; Drobny, G. *J. Magn. Reson.* **1985**, *61*, 306–320.

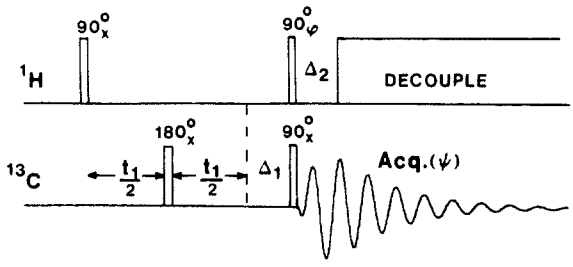

Figure 3. Pulse scheme of the simple phase-sensitive heteronuclear shift correlation experiment. Data accumulation is started immediately after the 90° ^{13}C pulse, at time Δ_2 before decoupling is started. The delay period Δ_1 is chosen to be an integer number, N, times the t_1 increment, in such a way that $\Delta_1 \sim 0.4/J$. Δ_2 is set equal to about $0.3/J$. Before Fourier transformation in the t_1 dimension, data are right shifted by N data points, to facilitate phasing in the F_1 dimension. The phase, ϕ, and the receiver reference phase, ψ, are cycled as $\phi = x, y, -x, -y$; $\psi = x, x, -x, -x$. Data in odd- and even-numbered scans are stored in separate memory locations and a hypercomplex Fourier transform[16-18] is used. If no such routine is available, the decoupler can be positioned at one side of the spectrum and phase cycling $\phi = x, -x$ and $\psi = x, -x$ used.[27] Additionally, CYCLOPS phase cycling can be used by incrementing the phase of all ^{13}C pulses and of the receiver by 90° upon completion of the regular phase cycle, described above.

taining this information, and the majority of the ring protons remained unassigned. For example, it appeared impossible to show the crucial indirect connectivity between H1 and H3a or between H13 and H5a. As pointed out previously,[21] the homonuclear relay experiment is rather inefficient at transferring magnetization via adjacent methylene sites with nonequivalent geminal protons.

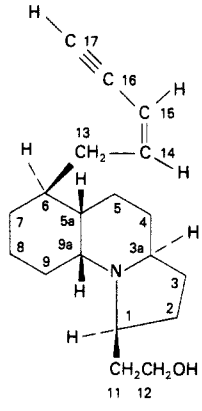

Heteronuclear Chemical Shift Correlation. The second step in the spectral analysis of GyTX is the recording of a heteronuclear chemical shift correlation spectrum.[23-25] Because of the limited amount of sample (8 mg) and the fact that only a 10-mm ^{13}C probe (with rather low sensitivity specifications) was available on the 500-MHz spectrometer, optimizing sensitivity of the shift correlation experiment was critical. Recording of an absorption mode heteronuclear shift correlation spectrum provides sensitivity higher by a factor of $\sqrt{2}$,[26] relative to the experiment where artificial phase modulation is induced,[24,25] and an absolute value mode calculation is made before display. Moreover, the higher resolution obtained in the absorption mode version is essential in the application to GyTx. We used the simplified version of the phase-sensitive pulse scheme,[27] as sketched in Figure 3. ^{13}C data acquisition is started immediately following the 90° ^{13}C pulse, at a time Δ_2 before ^1H decoupling is started. Correct phasing after the first Fourier transformation of the very low S/N spectra

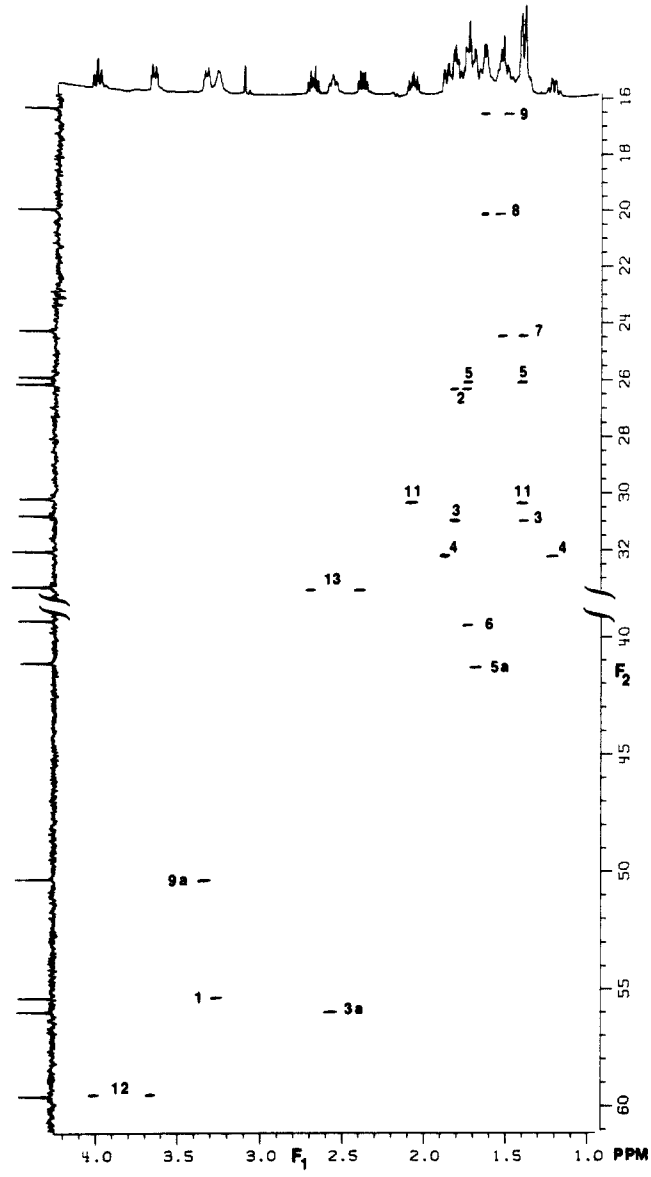

Figure 4. Absorption mode heteronuclear chemical shift correlation spectrum of GyTx, recorded at 125.8-MHz ^{13}C frequency. The spectrum results from 6 h of data accumulation. For comparison, the ^{13}C spectrum shown along the vertical axis was recorded in 15 min.

is obtained by using phasing parameters identical with those used for phasing a (higher S/N) FID spectrum for which the phase of the radio frequency pulse and the phase-sensitive detector are set identically (both x). Note that in the 2D pulse scheme of Figure 3 the ^{13}C pulse and phase detector are 90° out of phase relative to one another. After transposition of the 2D data matrix, $\Delta_1/\Delta t_1$ right shifts of the t_1 data are performed, prior to Fourier transformation (Δ_1 is the fixed delay period in Figure 3, and Δt_1 is the time between successive t_1 durations). This minimizes the linearly frequency dependent phase correction needed in the F_1 dimension and therefore facilitates correct phasing in this dimension. The base line distortion introduced by this procedure is not noticeable in this low-sensitivity 2D spectrum, and even if it were, it would not significantly affect peak positions. To further optimize the sensitivity of the experiment, we used a relatively long acquisition time in the t_2 dimension of 152 ms, the approximate decay constant of the ^{13}C signal. For the same reason, a relatively short sampling time in the t_1 dimension of 60 ms ($1/2J_{HH}$) was used, and no attempt was made to resolve the ^1H–^1H multiplet structure in the F_1 dimension.

The resulting phase-sensitive 2D ^1H–^{13}C correlation spectrum is shown in Figure 4. This spectrum provides direct assignment for all ^{13}C resonances for which the corresponding ^1H assignments

(22) Wagner, G. *J. Magn. Reson.* **1983**, *55*, 151–156.
(23) Maudsley, A. A.; Müller, L.; Ernst, R. R. *J. Magn. Reson.* **1977**, *28*, 463–470.
(24) Bax, A.; Morris, G. A. *J. Magn. Reson.* **1981**, *42*, 501–505.
(25) Bax, A. In "Topics in Carbon-13 NMR"; Levy, G. C., Ed.; Wiley: New York, 1985; Vol. 4, Chapter 8.
(26) Levitt, M. H. In "Two-Dimensional NMR and Related Techniques"; Brey, W. S., Ed.; Academic Press: New York, in press.
(27) Bax, A.; Sarkar, S. K. *J. Magn. Reson.* **1984**, *60*, 170–176.

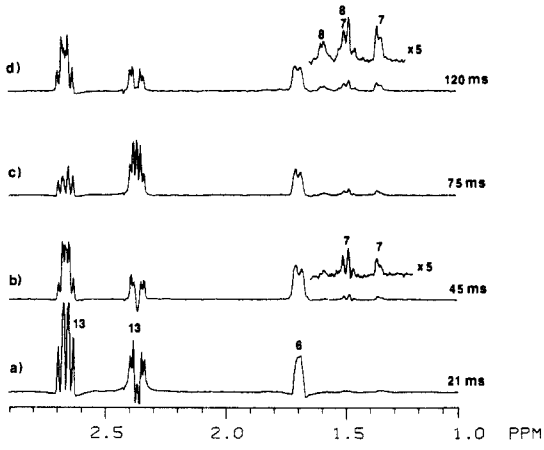

Figure 5. HOHAHA spectra obtained by transfer from the H13 multiplet at 2.38 ppm, for various durations of the propagation delay. Because of the relatively small couplings between H6 and the H7 protons, relatively long propagation times are needed before magnetization transfer to the H7 and H8 protons is observed. The downfield region of the spectra (not shown) contains resonances of protons H14, H15, and H17.

have been made. Additionally, assignment of C6 is possible because this is the only methine ^{13}C resonance that correlates with the frequency of H6, determined from the COSY spectrum (Figure 2). By default, the only remaining upfield methine carbon resonance is assigned to C5a.

Homonuclear Hartmann–Hahn Magnetization Transfer. The third step in the spectral analysis of GyTx is to use the recently proposed one-dimensional homonuclear Hartmann–Hahn (HOHAHA) method[7] to determine relayed connectivity. Although in principle the 2D version of this experiment[28] could be used, the one-dimensional version is more convenient if magnetization transfer is studied as a function of mixing time. Problems concerning the required measuring time, the data processing time, and the required disk storage space are greatly alleviated by using the 1D version. This 1D HOHAHA experiment is a difference method with the following pulse sequence: selective 180°(on/off)–90_x–$(SL_y$–60_{-y}–300_y–$SL_{-y}60_y$–$300_{-y})_n$–SL_y–acquire (add/subtract), where SL_y is a long spin lock pulse (in our case 3 ms). To protect the radio frequency electronics, reduced power (4 W) is used for all pulses but the selective 180° pulse. On our spectrometer, 4 W of radio frequency power generates a 6-kHz radio-frequency field strength. The spin lock field is phase-alternated along the $\pm y$ axis to minimize the effect of a small Hartmann–Hahn mismatch[29,30] that is caused by the different radio frequency offsets of the various spins and the consequently slightly different *effective* radio-frequency field strengths for coupled nuclei. The $60_y;300_{-y}$ pulse pair serves to minimize loss of spin locked magnetization during phase alternation of the spin lock field.[30] The homonuclear decoupler is used to generate the selective 180° pulse (duration of 50 ms), which inverts the multiplet of a preselected proton, A. After the following nonselective $90°_x$ pulse, the SL_y radio-frequency field locks the magnetization of spin A along the $-y$ axis and the magnetization of all other spins is locked along the y axis. The spin lock field provides a Hartmann–Hahn match[31] for coupled protons and causes net magnetization transfer from spin A to its coupled proton M, at a rate determined by the scalar coupling content J_{AM}; i.e., the spin locked component of M along the y axis will decrease if spin A is locked along the $-y$ axis. If M is coupled to a third proton, X (not coupled to A), the X spin magnetization will subsequently decrease because of the Hartmann–Hahn contact with spin M. For short mixing times, the difference spectrum will only show the selectively inverted

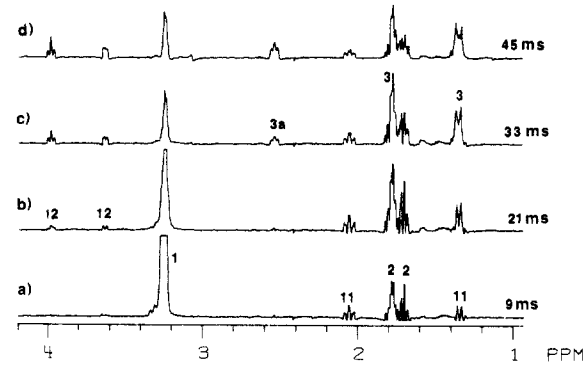

Figure 6. HOHAHA spectra obtained by transfer from the H1 multiplet, for various durations of the propagation period. Each spectrum results from 128 scans (4 min).

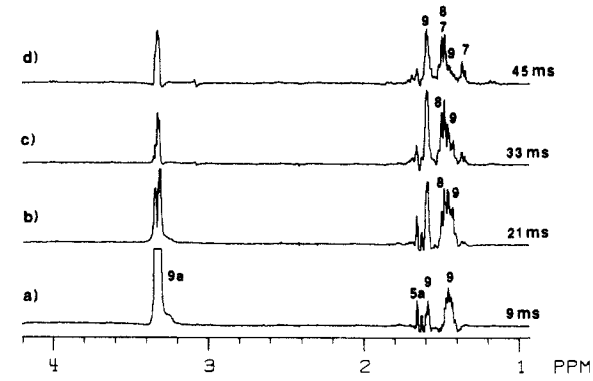

Figure 7. HOHAHA spectra obtained by transfer from the H9 multiplet, for various durations of the propagation period.

resonance, plus resonances of protons directly coupled to it. For longer mixing times, magnetization relay also occurs and more resonances will appear in the difference spectrum. The HOHAHA method is based on the concept of isotropic mixing[32–35] in the spin system that occurs if the Zeeman part of the Hamiltonian is annihilated.

As a first example, Figure 5a shows the HOHAHA difference spectrum obtained after selectively inverting proton H13 at 2.37 ppm and using a 21-ms total spin lock duration. During this short mixing period, magnetization has only propagated to its geminal partner (2.67 ppm) and to vicinal coupling partners H14 at 5.98 ppm (not shown) and H6 (1.71 ppm). For longer mixing times (Figure 5b), two additional multiplets appear in the high-field region of the spectrum, which are tentatively assigned to the H7 protons. H5a is assigned on the basis of Figure 4 and partially overlaps with H6. The H5a–H6 scalar coupling is apparently rather small, causing little transfer from H6 to H5a. For a mixing time of 120 ms (Figure 5d) a new resonance appears at 1.62 ppm, and the resonance at 1.52 ppm increases in intensity relative to the H7 multiplet at 1.37 ppm. On the basis of this and the heteronuclear shift correlation spectrum of Figure 4, we tentatively assign the ^1H resonances at 1.52 and 1.62 ppm to H8.

In a similar way, a second set of HOHAHA experiments is performed, starting the transfer from proton H1. For a short propagation period (9 ms) its direct coupling partners (H11, H11′, H2, and H2′) appear in the difference spectrum (Figure 6a). For longer mixing times (Figure 6c,d), a methine proton resonance appears at 2.55 ppm which then must be assigned to H3a. Since magnetization relay must have occurred via the geminal protons H3, these H3 resonances must be present in spectra b and c in

(28) Davis, D. G.; Bax, A. *J. Am. Chem. Soc.* **1985**, *107*, 2820–2821.
(29) Bax, A.; Davis, D. G. *J. Magn. Reson.* **1985**, *63*, 207–213.
(30) Bax, A.; Davis, D. G. In "Advanced Magnetic Resonance Techniques in Systems of High Molecular Complexity"; Nicolai, N., Valensin, G., Eds.; Birkhauser: Basel, in press.
(31) Hartmann, S. R.; Hahn, E. L. *Phys. Rev.* **1962**, *128*, 2042–2053.
(32) Weitekamp, D. P.; Garbow, J. R.; Pines, A. *J. Chem. Phys.* **1982**, *77*, 2870–2883.
(33) Caravatti, P.; Braunschweiler, L.; Ernst, R. R. *Chem. Phys. Lett.* **1983**, *100*, 305–310.
(34) Braunschweiler, L.; Ernst, R. R. *J. Magn. Reson.* **1983**, *53*, 521–528.
(35) Chandrakumar, N.; Subramanian, S. *J. Magn. Reson.* **1985**, *62*, 346–349.

Table I. ^{13}C and ^{1}H Chemical Shifts in GyTX

position	^{13}C shift (ppm)	^{1}H shift (ppm)
1	55.36	3.26
2	26.26	1.72; 1.80
3	30.93	1.36; 1.79
3a	55.95	2.55
4	32.16	1.18; 1.86
5	26.01	1.37; 1.71
5a	41.17	1.67
6	39.34	1.71
7	24.37	1.37; 1.50
8	20.04	1.52; 1.62
9	16.47	1.45; 1.62
9a	50.33	3.33
11	30.28	1.36; 2.07
12	59.53	3.65; 4.00
13	33.42	2.37; 2.67
14	145.00	5.98
15	109.32	5.49
16	80.31	
17	81.41	3.08

Figure 6. The two multiplets at 1.35 and 1.79 ppm have notably increased in intensity relative to the other two upfield multiplets. This suggests that the two H3 multiplets are located at these positions. Inspection of the heteronuclear chemical shift correlation spectrum confirms the presence of a pair of geminal protons at these positions. From the COSY spectrum (Figure 2) it is seen that the most upfield multiplet (1.18 ppm) is coupled to H3a and this resonance therefore must be assigned to H4. The heteronuclear shift correlation spectrum then identifies carbon C4 (32.2 ppm) and the other H4 proton (1.86 ppm).

Spectral assignment is completed by a third set of HOHAHA experiments, transferring from the multiplet at 3.33 ppm, which after assignment of H3a must be assigned to H9a. For a short mixing period, magnetization is transferred to H5a and geminal protons H9 (1.62 and 1.45 ppm) (Figure 7a). After H5a is assigned from the heteronuclear shift correlation spectrum, the H9 resonances can also be identified from the COSY spectrum via correlation with H9a. For longer mixing times, resonances of H8 and H7 appear (Figure 7b,c), confirming the earlier tentative assignments of these resonances. Finally, protons H5 are most readily assigned from the COSY spectrum via correlation with H4 and resonate at 1.37 and 1.71 ppm. Correlation with the ^{13}C shifts (Figure 3) completes the assignment. The ^{1}H and ^{13}C shifts are presented in Table I.

Discussion

The present investigation of a complex frog alkaloid illustrates the power of 2D homo- and heteronuclear shift correlation and of the related HOHAHA experiment. A number of other 2D NMR experiments[36-42] are intrinsically even more powerful for spectral assignment and structure determination than the methods discussed in this paper. Unfortunately, all these more sophisticated experiments have much lower sensitivity than the methods discussed here and could not be used for the study of the limited sample quantity available. For the GyTx sample, the average ^{1}H relaxation time, T_1, at 500 MHz is slightly longer than for the ^{13}C nuclei. Consequently, there is no advantage in using ^{13}C polarization enhancement with INEPT[43,44] or DEPT[45,44] type techniques. It took 6 h to record the shift correlation spectrum of Figure 3 vs. 15 min for a regular optimized ^{13}C FID spectrum (with NOE) of 9:1 signal-to-noise ratio. The sensitivity in the 2D ^{1}H-^{13}C correlation spectrum is usually lowest for the methylene sites with nonequivalent geminal protons because the ^{13}C intensity is spread over two multiplets in the F_1 dimension. Because these geminal protons generally have the shortest T_1 value, the delay time between the end of data acquisition and the first 90° ^{1}H decoupler pulse should be optimized for this short T_1 value. We used a delay time of 1.8 s, corresponding to 1.5 times the T_1 value of the geminal protons.

The sensitivity issue is usually less important in homonuclear ^{1}H experiments. Instead, here the obtainable resolution is the critical issue. Again, recording of phase-sensitive absorption mode 2D spectra is useful for optimizing resolution. For this reason we have used the phase-sensitive double-quantum filtered version[9] of the COSY experiment. Complete phase cycling, needed to suppress artifacts, requires 64 steps per t_1 increment and quadruples the minimum measuring time relative to an absolute value mode experiment. Nevertheless, the higher resolution more than compensates for this increase in measuring time.

The one-dimensional HOHAHA experiments are most useful for establishing relayed and multiple relayed connectivity. For longer mixing times, the magnetization of the selectively inverted spin gets distributed over an increasing number of protons, proportionally decreasing the intensity in the difference spectrum. Also, this technique is a difference method and since only experiments in which the selected ^{1}H multiplet is inverted (odd-numbered scans) contribute to the final spectrum, signal to noise is reduced by another factor of 2. Nevertheless, high-sensitivity spectra can be obtained in several minutes. The interpretation of HOHAHA spectra as a function of mixing time is relatively straightforward: for longer mixing times magnetization propagates further away from the selectively inverted proton. The rate of propagation depends on the size of the scalar coupling and on the number of interacting protons. Transfer via methylene protons, for example H1 to H3a, generally occurs much faster than transfer via a methine proton, for example, H13 to H7. The HOHAHA experiment relies on the same physical mechanism as the TOCSY experiment, proposed by Braunschweiler and Ernst.[34] As they and others[16,31,46] have pointed out, there is also antiphase magnetization (perpendicular to the spin lock field) involved in the transfer of net magnetization between spins. This generates phase distortions within the individual ^{1}H spin multiplets and prohibits a precise measurement of ^{1}H-^{1}H coupling constants from HOHAHA difference spectra. Alternative methods that may permit the measurement of coupling constants from HOHAHA spectra are currently under investigation.

The approach described in this paper is applicable to a large number of NMR assignment problems. In cases where sufficient sample and instrument time are available, other more advanced heteronuclear experiments[37-40] and homonuclear ^{13}C techniques[36,41,42] may be more straightforward to use for this purpose. If insufficient sample is available for recording a heteronuclear chemical shift correlation spectrum, indirect detection of the ^{13}C via the ^{1}H signals can alleviate this problem by at least an order of magnitude.[47-52] The inherent sensitivity of the double-quantum filtered COSY method and of the HOHAHA experiment is

(36) Bax, A.; Freeman, R.; Frenkiel, T. A.; Levitt, M. H. *J. Magn. Reson.* **1981**, *43*, 478-483.
(37) Bolton, P. H.; Bodenhausen, G. *Chem. Phys. Lett.* **1982**, *89*, 139-144.
(38) Kessler, H.; Bernd, M.; Kogler, H.; Zarbock, J.; Sorensen, O. W.; Bodenhausen, G.; Ernst, R. R. *J. Am. Chem. Soc.* **1983**, *105*, 6944-6952.
(39) Kessler, H.; Griesinger, C.; Zarbock, J.; Loosli, H. R. *J. Magn. Reson.* **1984**, *57*, 331-336.
(40) Bax, A.; Davis, D. G.; Sarkar, S. K. *J. Magn. Reson.* **1985**, *63*, 230-234.
(41) Bax, A.; Freeman, R.; Frenkiel, T. A. *J. Am. Chem. Soc.* **1981**, *103*, 2102.
(42) Bhacca, N. S.; Balandrin, M. F.; Kinghorn, A. D.; Frenkiel, T. A.; Freeman, R.; Morris, G. A. *J. Am. Chem. Soc.* **1983**, *105*, 2538-2543.
(43) Morris, G. A.; Freeman, R. *J. Am. Chem. Soc.* **1979**, *101*, 760-761.
(44) Sorensen, O. W.; Ernst, R. R. *J. Magn. Reson.* **1983**, *51*, 4477-4489.
(45) Doddrell, D. M.; Pegg, D. T.; Bendall, M. R. *J. Magn. Reson.* **1982**, *48*, 323-327.
(46) Chingas, G. C.; Garroway, A. N.; Bertrand, R. D.; Moniz, W. B. *J. Chem. Phys.* **1981**, *74*, 127-156.
(47) Müller, L. *J. Am. Chem. Soc.* **1979**, *101*, 4481-4484.
(48) Bax, A.; Griffey, R.; Hawkins, B. L. *J. Magn. Reson.* **1983**, *55*, 301-315.
(49) Bendall, M. R.; Pegg, D. T.; Doddrell, D. M. *J. Magn. Reson.* **1983**, *52*, 81-117.
(50) Bodenhausen, G.; Ruben, D. J. *Chem. Phys. Lett.* **1980**, *69*, 185.
(51) Bax, A.; Griffey, R.; Hawkins, B. L. *J. Am. Chem. Soc.* **1983**, *105*, 7188-7190.
(52) Live, D. H.; Davis, D. G.; Agosta, W. C.; Cowburn, D. *J. Am. Chem. Soc.* **1984**, *106*, 6104-6105.

sufficient for use on submilligram quantities.

Experimental Section

NMR experiments were carried out on a Nicolet 500-MHz spectrometer, equipped with a 10-mm ^{13}C probe and a 5-mm ^{1}H probe. Eight milligrams of sample were dissolved in 0.4 mL of $^{2}HCCl_3$, and a 5-mm Wilmad-528pp sample tube was used throughout. All spectra were recorded at 25 °C. ^{13}C shifts are indirectly referenced to tetramethylsilane (Me_4Si) by using the central line of the $^{2}HCCl_3$ triplet as an internal reference (77.0 ppm). ^{1}H shifts are relative to a small amount of internal Me_4Si.

Double-Quantum Filtered COSY. t_1 values (480) ranging from 0 to 175 ms were used and two FID's consisting of 512 *complex* data points each were acquired per t_1 value. The acquisition time in the t_2 dimension was 188 ms. Data were zero-filled in both dimensions, to yield a 1024 × 1024 data matrix for the absorptive part of the 2D spectrum. Gaussian line broadening was used in both dimensions to avoid truncation. The phase cycling of the 90_ϕ–t_1–90_ψ–90_θ–acq.(t_2) sequence was the following:

ϕ: $x, y, -x, -y, x, y, -x, -y, x, y, -x, -y, x, y, -x, -y$

ψ: $x, x, x, x, x, x, x, x, x, x, x, x, x, x, x, x$

θ: $x, x, -x, -x, y, y, -y, -y, -x, -x, x, x, -y, -y, y, y$

acq.: $x, x, x, x, -y, -y, -y, -y, -x, -x, -x, -x, y, y, y, y$

Additionally, CYCLOPS phase cycling[53] was used by repeating the entire 16-step experiment four times with the phases of all radio-frequency pulses and of the receiver incremented by 90° each time. The delay time between scans (including the data acquisition time, t_2) was 1.98 s and the total data accumulation time was 17 h. Small artifacts on the lines $F_1 = NF_2$ ($N = -2, -1, 0, 1, 2$) are due to an insufficiently long delay period between scans ($\sim T_1$). For longer delay periods these artifacts rapidly decrease in intensity, but this requires unacceptably long data accumulation times.

^{1}H–^{13}C Heteronuclear Chemical Shift Correlation. t_1 values (100) ranging from 0 to 59.4 ms were used and two FID's consisting of 1024 *complex* data points each were acquired per t_1 value. The acquisition time in the t_2 dimension was 152 ms. Data were zero-filled in both dimensions, to yield a 2048 × 512 data matrix for the absorptive part of the 2D spectrum. Gaussian line broadening was used in both dimensions to avoid truncation. Ninety six scans were acquired per t_1 value and a delay time of 1.8 s was used between the end of data acquisition and the 90° pulse of the next scan. The total measuring time was 6 h.

HOHAHA Experiments. Each of the HOHAHA spectra results from 128 accumulations (~4 min). A 10-Hz decoupler radio frequency field strength (50 ms 180° pulse) was used to selectively invert the ^{1}H multiplet of interest. A tuned Henry class A radioamplifier was used to generate 4-W radio-frequency power for the observe channel, corresponding to a 6-kHz radio-frequency field strength. Tuned diodes and a band-pass filter were used in the transmitter line to avoid sensitivity loss and to prevent perturbation of the ^{2}H lock channel by the long spin-lock pulse. To avoid poor cancellation in the difference spectra, the sample was not spun.

Acknowledgment. We thank Dr. John Daly for risking his skin in the South American rain forest, collecting the frog skins from which GyTx was extracted. We are also indebted to Rolf Tschudin for continuous technical support and to Dr. Donald Davis for useful suggestions concerning the purification of the sample. Dr. Laura Lerner made many helpful comments during the preparation of the manuscript.

(53) Hoult, D. I.; Richards, R. E. *Proc. R. Soc. London, Ser. A* **1975**, *344*, 311.

Theoretical Study of the Addition of Hydrogen Halides to Olefins: Reaction of Dimeric Hydrogen Fluoride with Ethylene

Carmen Clavero, Miquel Duran, Agustí Lledós, Oscar N. Ventura,† and Juan Bertrán*

Contribution from the Departament de Química Física, Universitat Autònoma de Barcelona, Bellaterra (Barcelona), Spain. *Received July 10, 1985*

Abstract: This paper presents a theoretical study of the addition of $(HF)_2$ to ethylene using ab initio methods with the 3-21G basis set. Thermodynamical calculations to obtain ΔG°_{298} values were also made. Comparison with the bimolecular addition of HF to ethylene shows a larger stabilization of the transition state obtained, reflected in a decrease of the potential barrier. This fact, along with an analysis of the energy components and the mechanism, allows us to assert the catalytic activity of the second HF molecule. From the thermodynamics of the reaction, the need for a "bimolecular" collision between $(HF)_2$ and ethylene and not a termolecular one is deduced, and the ability of this mechanism to explain data in the gas phase and in nonpolar solvents is sustained.

Addition of hydrogen halides to olefins belongs to the classic reactions of organic chemistry. It is generally accepted that three distinct pathways are possible in those processes, although not all of them are applicable to all olefins and all hydrogen halides. The first one, ionic addition, takes place in polar solvents and is assumed to proceed through protonation, yielding a carbonium intermediate that later evolves to the product.[1] This is always a normal Markovnikov addition. The second mechanism, present only in HBr additions,[2] is the anti-Markovnikov addition, usually explained by the so-called peroxide effect,[3] which suggests a radical chain mechanism,[4] and has been verified in the gas phase and in solution. Finally, we have the direct bimolecular addition, which occurs in gas phase, that is, the reverse of the much-studied elimination of HX from haloalkanes by pyrolisis; it has been examined in detail in the case of hydrogen iodide reaction with olefins.[5]

In nonpolar solvents without radical initiators, experimental facts seem not to be explainable by any of the aforementioned

† Permanent address: Cátedra de Quimica Cuántica, Facultad de Quimica, Montevideo, Uruguay.

(1) De la Mare, P. B. D.; Bolton, R. "Electrophilic Additions to Unsaturated Systems"; Elsevier: New York, 1961; p 55 FF.
(2) Pryor, W. A. "Free Radicals"; McGraw-Hill: New York, 1966; p 212.
(3) (a) Kharasch, M. S.; Mayo, F. R. *J. Am. Chem. Soc.* **1933**, *55*, 2468–2496. (b) Hey, D. H.; Waters, W. O. *Chem. Rev.* **1937**, *21*, 169–208.
(4) (a) Stacey, F. W.; Harris, J. F. In "Organic Reactions"; Cope, A. C., Ed.; Wiley: New York, 1963; Vol. 13, p 91. (b) Abell, P. I. In "Free Radicals"; Wiley: New York, 1973; Vol. 2, p 63.
(5) Benson, S. W.; Bose, A. N. *J. Chem. Phys.* **1963**, *39*, 3463–3473.

0002-7863/86/1508-0923$01.50/0